Laboratory investigation of the acoustic response of seagrass tissue in the frequency band 0.5–2.5 kHz

Preston S. Wilson[a)]
Department of Mechanical Engineering and Applied Research Laboratories, The University of Texas at Austin, Austin, Texas 77712-0292

Kenneth H. Dunton
Marine Science Institute, The University of Texas at Austin, Port Aransas, Texas 78373-5015

(Received 2 October 2007; revised 29 January 2009; accepted 30 January 2009)

Previous *in situ* investigations of seagrass have revealed acoustic phenomena that depend on plant density, tissue gas content, and free bubbles produced by photosynthetic activity, but corresponding predictive models that could be used to optimize acoustic remote sensing, shallow water sonar, and mine hunting applications have not appeared. To begin to address this deficiency, low frequency (0.5–2.5 kHz) acoustic laboratory experiments were conducted on three freshly collected Texas Gulf Coast seagrass species. A one-dimensional acoustic resonator technique was used to assess the biomass and effective acoustic properties of the leaves and rhizomes of *Thalassia testudinum* (turtle grass), *Syringodium filiforme* (manatee grass), and *Halodule wrightii* (shoal grass). Independent biomass and gas content estimates were obtained via microscopic cross-section imagery. The acoustic results were compared to model predictions based on Wood's equation for a two-phase medium. The effective sound speed in the plant-filled resonator was strongly dependent on plant biomass, but the Wood's equation model (based on tissue gas content alone) could not predict the effective sound speed for the low irradiance conditions of the experiment, in which no free bubbles were generated by photosynthesis. The results corroborate previously published results obtained *in situ* for another seagrass species, *Posidonia oceanica*. © *2009 Acoustical Society of America.*
[DOI: 10.1121/1.3086272]

PACS number(s): 43.30.Ma [KGF] Pages: 1951–1959

I. INTRODUCTION

The acoustical characteristics of seagrass beds are important in a number of naval, commercial, and ecological applications. Gas-filled channels (aerenchyma) within the seagrass plants and gas bubbles generated by the plants during photosynthesis dominate their acoustic behavior and numerous studies have demonstrated and analyzed significant acoustic effects due to this acoustic contrast with the water and ocean bottom. For example, mine hunting performance is severely reduced in seagrass meadows. McCarthy and Sabol[1] attempted to locate a Manta target simulator (an inert version of a Manta naval mine) that was deployed in a meadow of *Zostera marina* using two commercial side scan sonars operating at both 100 and 500 kHz. Neither sonar was able to detect the target in numerous attempts. Similarly, a hand-held mine hunting sonar deployed by divers and operating in the 115–140 kHz frequency range was unable to detect the target.[1] Backscatter from the seagrass was sufficiently strong to completely obscure reflections from the Manta target simulator.

Since shallow water sonar performance can be severely limited by reverberation, Lyons and Abraham[2] studied the variation in seafloor reverberation level at 80 kHz in the presence of *Posidonia oceanica* near Sardinia and Sicily. They found that the mean seafloor backscatter strength in the presence of seagrass was about 10 dB higher across a range of grazing angles than compared to a sand-covered bottom and varied between 0 and 8 dB higher than a mud bottom, depending on grazing angle. While the mean backscatter strength was not uniquely related to the bottom characteristics, they found that a combination of mean backscatter strength and a statistical description of the variability of the backscatter could potentially characterize the bottom. The variability was attributed to the inhomogeneous distribution of *Posidonia* density and the motion of leaves due to swell or currents.

Seagrass meadows serve as habitat for many economically important estuarine organisms. The same acoustic characteristics that obscure mines and hinder sonar performance can potentially be used to assess the ecological condition and the extent of this valuable littoral ecosystem. Consequently, acoustic remote sensing methods are under development to exploit these characteristics.[3] Side scan sonar has been used extensively for imaging seagrass beds and as a possible management tool for littoral ecosystems.[4] An extensive comparison between seagrass mapping by side scan sonar and by aerial photography was conducted by Mulhearn.[5] Komatsu *et al.*[6] showed that plant-occupied volume can be extracted from the three-dimensional images produced by multi-beam side scan sonar. Finally, Hermand[3] conducted extensive studies over the past decade on the acoustic remote sensing of seagrass photosynthesis using frequencies ranging from 0.1 to 16 kHz. One study[7] on *Posidonia oceanica* was conducted

[a)]Electronic mail: pswilson@mail.utexas.edu

in the frequency range 0.1–1.6 kHz, which overlaps the frequency range used in this work. Photosynthetic activity produces free gas bubbles on the plants and in the water column which affects the local sound speed and hence the waveguide impulse response. Hermand's technique relies on monitoring the acoustic impulse response between two locations in a shallow water waveguide and inverting for a measurement of oxygen productivity.

In all the applications described above, accurate predictive models that relate the physical characteristics of plant anatomy, density, and photosynthetic activity to the acoustic scattering and propagation response could potentially be used to (1) infer target and ecological parameters from acoustic sonar and remote sensing signals and (2) improve and optimize acoustic image formation for mapping and target identification. As a first step toward the development of such models, the hypothesis that the acoustic behavior of immersed plant leaves or rhizomes can be considered an effective medium dominated by internal plant gas content was investigated. Photosynthetically produced gas bubbles attached to tissue surfaces or in the water surrounding the plants were excluded. Low frequency (0.5–2.5 kHz) laboratory experiments were conducted on three freshly collected species: *Thalassia testudinum* (turtle grass), *Syringodium filiforme* (manatee grass), and *Halodule wrightii* (shoal grass). This frequency range is directly applicable to the remote sensing application of Hermand[3] and Hermand *et al.*[7] but is significantly lower than the frequencies used in side scan sonar studies and object detection applications. Despite this discrepancy, the frequency range used in the present study is an appropriate starting point for the investigation of the fundamental physics of a fluid-loaded gas-bearing structure such as seagrass tissue because at sufficiently low frequencies, below the resonance frequency of any individual gas-filled cavity, the relative acoustic importance of the gas content compared to the tissue can be assessed through the use of an effective medium model, such as Wood's equation.[8] This study is not intended to lead directly to a model of propagation and scattering in the presence of seagrass in the frequency range of side scan and mine hunting sonar systems, but is instead intended to yield basic insight into the acoustic behavior of seagrass tissue.

A one-dimensional acoustic resonator technique was used to assess the biomass and effective acoustic properties of individual leaves and rhizomes. Independent biomass and gas content estimates were gathered using macro- and microscopic tissue imagery. The acoustic results were compared to model predictions based on Wood's equation[8] for a two-phase medium. The effective sound speed in the plant-filled resonator was strongly dependent on plant biomass, but the Wood's equation model (based on gas content alone) was unable to describe the effective sound speed for the low irradiance conditions of the experiment, in which no free bubbles were generated by photosynthesis. These laboratory results corroborated findings obtained *in situ* for another seagrass species, *Posidonia oceanica*.[3]

II. LOW FREQUENCY ACOUSTIC RESPONSE AND PLANT BIOMASS

Seagrass leaves and rhizomes contain internal gas-filled channels (aerenchyma)[9] and during photosynthesis, gas bubbles produced by the plant are found attached to external surfaces. This study was focused on the effects of the aerenchyma on the acoustic response characteristics; hence the experiments were done in sufficiently low light conditions to prevent external bubble formation. The following hypotheses were investigated: (1) the acoustic response is dominated by the gas within the aerenchyma and (2) seagrass tissues, when gas-free, possess acoustic properties close to those of water. Under these assumptions, the contents of the acoustic resonator (seawater and plants) were considered to be an effective acoustic medium composed of a liquid seawater phase and a gas phase, as is done for air bubbles in water.

The speed of sound in this medium is a strong function of the gas content, or void fraction, which is defined as $\chi = V_{\text{gas}}/V_{\text{tot}}$. The volume of gas in the aerenchyma is V_{gas} and the total volume of the resonator is V_{tot}. If the frequency of the acoustic excitation is well below the resonance frequency of the largest gas cavity, then the effective medium sound speed c_{eff} is given by Wood's equation[8]

$$\frac{1}{c_{\text{eff}}^2} = \frac{(1-\chi)^2}{c_\ell^2} + \frac{\chi^2}{c_g^2} + \chi(1-\chi)\frac{\rho_g^2 c_g^2 + \rho_\ell^2 c_\ell^2}{\rho_\ell \rho_g c_\ell^2 c_g^2}, \tag{1}$$

where the subscripts ℓ and g refer to the liquid and gas phases, respectively, c_i is the intrinsic sound speed of phase i, and ρ_i is the density of phase i. If hypotheses (1) and (2) are true, then the sound speed observed inside the resonator should be directly related to the aerenchyma gas volume via Eq. (1) and also related to the plant biomass. In this study, leaf and rhizome volume was used to represent the biomass. The exact composition of the gas inside the aerenchyma is not known. Since it must contain oxygen and potentially nitrogen, the gas was considered to be air. The density difference between oxygen and nitrogen leads to a sound speed difference between the pure gases of about 7%, but this was found to be negligible in comparison to other sound speed effects observed in this study. The sound speed for air (315 m/s) originally cited by Wood was used,[8] which is appropriate for air bubbles in water at the surface.[10]

III. EXPERIMENT

Acoustical response trials were conducted *in vitro* using a one-dimensional acoustic resonator (Fig. 1) constructed from transparent polyvinyl chloride (PVC) schedule 40 pipe of circular cross-section (60 ± 0.5 mm outer diameter and 4.2 ± 0.2 mm wall thickness) and with length $L = 401 \pm 1$ mm. The cylinder was filled with fresh seawater from the Gulf of Mexico that had spent several hours in an outdoor settling tank to minimize interference from suspended particulates. Seagrass leaves or rhizomes were placed in the resonator (additional details about the plant tissue preparation are provided below). The air-water interface at the top and a Styrofoam block at the bottom of the cylinder provided pressure release acoustic boundary conditions to a high degree of approximation, as described in Ref. 11.

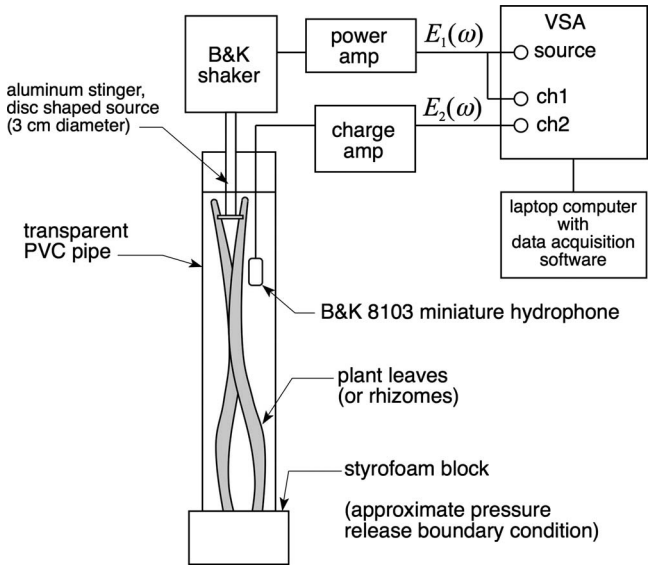

FIG. 1. The acoustic resonator and the measurement instrumentation are shown.

Acoustic standing waves were generated with a 3-cm-diameter aluminum piston that was attached to an electromechanical shaker via an aluminum stinger. Band-limited periodic chirps were produced by a vector signal analyzer (VSA) and directed to the shaker through a power amplifier. The source signal was also digitized by the VSA. The piston was positioned a few centimeters below the air-water interface. The acoustic pressure inside the resonator was received with a miniature hydrophone, positioned a few centimeters below the source. The received signals were amplified with a charge amplifier, band-pass filtered (10 Hz–10 kHz), and digitized by the VSA. According to manufacturer specifications, the source velocity response was flat to within less than ± 1 dB in the experimental frequency range.

Relative acoustic pressure spectra y were then calculated onboard the VSA by way of a transfer function $y = P(\omega)/E_1(\omega) = [E_2(\omega)/M]/E_1(\omega)$, which yields the acoustic pressure $P(\omega)$ per unit voltage input $E_1(\omega)$ (see Fig. 1). The hydrophone system sensitivity M was used to convert the voltage $E_2(\omega)$ measured at the output of the charge amplifier into an acoustic pressure $P(\omega)$. According to the manufacturer's calibration, M varied less than ± 1 dB within the experimental frequency range and it was taken to be a constant. The spectra were calculated using 1601 frequency bins, 1.5 Hz resolution bandwidth, and 20 spectral averages, as defined by Eqs. (24)–(27) of Ref. 12. The use of a transfer function measurement preserved the phase of the acoustic pressure relative to the excitation signal and yielded the coherence function. The number of averages and the amplitude of the excitation were chosen to achieve a near-unity coherence function at all frequencies of interest, which guaranteed a high signal-to-noise ratio and ensured linear behavior.[13] Peak pressures inside the resonator were typically less than 170 dB re 1 μPa.

Live plants were collected intact with sediment cores from the Gulf of Mexico near the Marine Science Institute (MSI) in Port Aransas, TX and transported in seawater to MSI. *Thalassia* plants were collected on 9 November 2005, and *Halodule* and *Syringodium* plants were collected on 14 August 2007. The living plant cores were stored in transparent cylindrical chambers filled with seawater for 12–24 h between collection and the acoustic measurements. Previous work has shown that this artificial environment causes no detrimental effects on the plants within 5 days of collection.[14] The experimental protocol described below refers specifically to the preparation of leaves, but the same procedures were followed for rhizomes. The desired number of leaves was first removed from a plant by hand, rinsed of sediment in a seawater bath, and then transferred to the acoustic resonator, all without exposing the leaves to the air. No direct lighting was used. Only the diffuse fluorescent lighting present in the laboratory was incident upon the plants and no photosynthetic gas production expressed through external bubble formation was observed during the experiments. Hence these experiments represent a baseline case, corresponding to a minimum level of photosynthetic activity. It is known that the plant gas content and external bubble formation are a function of photosynthetic activity,[3] but variation in the illumination level was not included in this study.

The acoustic pressure spectra were then obtained as described above. The temperature of the water within the resonator was measured with a thermocouple gauge and ranged from 20.5 to 25.6 °C, depending on the time of day at which the seawater was drawn from the outdoor settling tank. The salinity was measured with a refractometer and remained constant throughout the experiments at 30 ppt. Temperature and salinity measurements were used to calculate the density and sound speed of the water using the UNESCO International Equation of State.[15] The mean water temperature near Port Aransas, TX, where these plants were collected, ranges from 13 to 30 °C over the course of the year;[16] hence the laboratory temperatures are within the range encountered in nature.

The leaves were removed from the resonator, laid flat on a table, and photographed alongside a machinist's scale. The surface area S of each leaf was measured using image analysis software. The thickness t was measured by imaging approximately five excised cross-sections from each leaf with a video microscope. The volume V_{leaf} of each leaf was then obtained from $V_{\text{leaf}} = S \times \bar{t}$, where $\bar{t}$ is the mean thickness of each leaf. Since the rhizomes of all three species and the leaves of *Syringodium* are circular in cross-section, their volumes were calculated from length (l) and the projected area (S_p) measurements using image analysis software; rhizome or leaf volume was calculated from $V = \pi S_p^2/4l$.

The leaf void fraction was obtained from image analysis that was performed on microscopic leaf cross-sections from the literature,[17] but no such cross-section images were found in the literature for the rhizomes. Digital cross sectional images of rhizomes were obtained using a microscope with backlighting. In both cases, image analysis was used to obtain the total area of the cross-section A_{tot} and the combined area of all the pores A_p within the cross-section (which are distinct in the images). Since the cross-sections are nearly uniform in the direction normal to the plane of the cross-

TABLE I. A different resonator tube was used for each seagrass species. The physical properties used in the evaluation of the elastic waveguide model for each resonator are shown. For all three, the resonator tube material was schedule 40 PVC pipe. When two entries appear within a cell, they are for the rhizomes and leaves, respectively.

	Thallasia	*Syringodium*	*Halodule*
Seawater sound speed, c_0 (m/s)	1517	1521	1517, 1519
Seawater density, ρ_1 (kg/m^3)	1020.9	1019.4	1017.3
Seawater temperature (°C)	20.5	25.6	22, 23
Air sound speed, c_g (m/s)	315	315	315
Air density, ρ_g (kg/m^3)	1.21	1.21	1.21
PVC comp. sound speed, c_l (m/s)	2030	2020	2020
PVC Poisson's ratio, ν	0.38	0.38	0.38
PVC density, ρ_w (kg/m^3)	1330	1330	1330
Inner wall radius, b (cm)	2.58	2.60	2.60
Outer wall radius, d (cm)	3.06	3.01	3.01

section images, the leaf void fractions were obtained with $\chi_{\text{leaf}}=V_{\text{air}}/V_{\text{leaf}}=A_p l/A_{\text{tot}} l=A_p/A_{\text{tot}}$. The same was done for the rhizomes. The existence of the leaf cross-sections in the literature was fortunate because sectioning the leaf tissue without causing visible damage to the leaf structure was difficult. The structures inside the leaves are generally smaller than the structures inside the rhizomes, and the leaf tissue is also softer than the corresponding rhizome tissue and tears more easily. Variation in leaf and rhizome internal void fraction within the species is possible, but to the author's knowledge, this has not been quantified in the literature.

IV. ELASTIC WAVEGUIDE EFFECT

In a gas-filled acoustic resonator, the walls are effectively rigid. In a liquid-filled resonator, there is significant coupling between the fill-liquid and the resonator walls. The result is a reduced sound speed relative to that observed in an unconfined environment. This effect is hereafter referred to as the elastic waveguide effect. An exact analytic model[18] for sound propagation in a finite-thickness elastic-walled, fluid-filled cylindrical tube was used to relate the speeds observed in the resonator to the intrinsic sound speed the material would exhibit in an unconfined environment. This procedure (and its validity) is discussed in Ref. 11 and summarized here. Equation (A1) of Ref. 11 is the dispersion relation for the resonator waveguide. The intrinsic (free-field) sound speed c_0 of the material that fills the resonator is an input parameter to Eq. (A1). The phase speed c_{ph} of the resonator's plane wave mode is an output. The resonator measurements described here yield the effective phase speed c_{eff} observed inside the resonator. The intrinsic sound speed c_0 is then varied in Eq. (A1) until the model output c_{ph} matches the measured value c_{eff}. The value of c_0 that achieves the match is reported as the effective sound speed that the material inside the resonator (seawater and plants) would exhibit in the ocean.

Three replicate resonator tubes were used in this work. The physical parameters needed for the elastic waveguide model [Eq. (A1), Ref. 11] are given in Table I. The sound speeds for the tube walls were initially calculated from the PVC manufacturer's specifications, but the values that were ultimately used (and reported in Table I) were obtained via a calibration procedure that utilized distilled degassed fresh water. With the internal liquid properties and the wall density known, the longitudinal sound speed in the wall was varied in the elastic waveguide model until the predicted phase speeds matched the speed measured during the calibration. There was about a 0.5% difference in phase speeds exhibited by the three resonator tubes when filled with distilled degassed water.

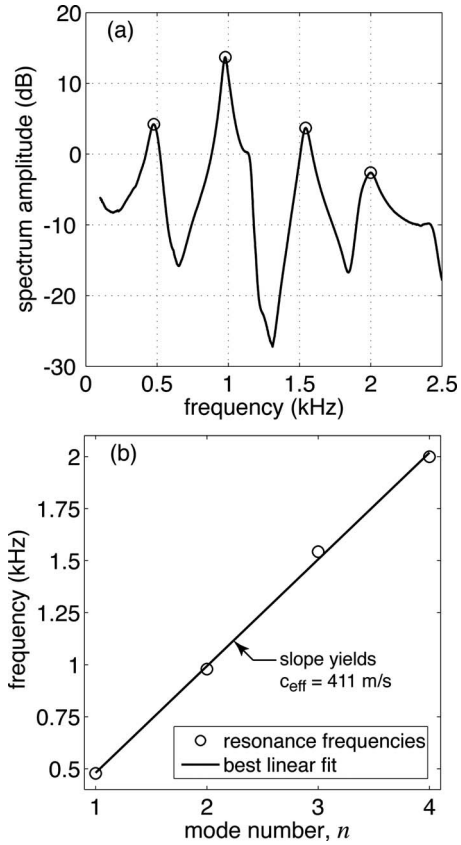

FIG. 2. A typical resonator spectrum (a) for three *Thalassia* leaves. Four resonance peaks are identified. The resulting best-fit sound speed is shown in (b).

V. RESULTS AND DISCUSSION

A typical spectrum from the resonator, obtained with three *Thalassia* leaves, is shown in Fig. 2(a). Four resonance frequencies were identified. The effective sound speed c_{eff} inside the water-and-leaf-filled resonator is inferred from the slope of the curve [Fig. 2(b)], which is the least-squares linear fit to the measured resonance frequencies. The nth resonance frequency is given by $f_n=(c_{\text{eff}}/2L)n$, where L is the length of the water column inside the resonator. Increased leaf biomass inside the resonator (adding additional leaves) shifts the spectrum toward lower resonance frequencies, which indicates a lower effective sound speed and clearly demonstrates that seagrass abundance is directly correlated with an acoustic parameter suitable for remote sensing.

Sound speeds c_{eff} (inferred from the resonance frequencies), free-field sound speeds c_0 (after correction for the elastic waveguide effect), and the apparent void fraction inside the resonator [see Eq. (1)] are reported in Table II. Biomass

TABLE II. Measured resonator sound speeds, associated free-field sound speeds, and apparent resonator void fractions are presented for *Thalassia testudinum*, *Syringodium filiforme*, and *Halodule wrightii*. Also shown are the acoustic- and image-based leaf and rhizome void fractions. The acronym VF is used for "void fraction."

Thalassisa testudinum				
No. of leaves, m	0	3	6	9
Resonator sound speed, c_{eff} (m/s)	422	411	396	393
Free-field sound speed, c_{o} (m/s)	1516	1176	909	874
Apparent acoustic resonator VF, $V_{\text{air}}/V_{\text{tot}}$	0	3.39×10^{-5}	9.12×10^{-5}	1.03×10^{-4}
Acoustically-determined leaf VF	$\chi_{\text{leaf,a}}=0.034$			
Image-based leaf VF	$\chi_{\text{leaf}}=0.23$			
No. of rhizomes, m	0	3	6	
Resonator sound speed, c_{eff} (m/s)	421	409	402	
Free-field sound speed, c_{o} (m/s)	1517	1022	918	
Apparent acoustic resonator VF, $V_{\text{air}}/V_{\text{tot}}$	0	6.13×10^{-5}	8.84×10^{-5}	
Acoustically-determined rhizome VF	$\chi_{\text{rhiz,a}}=0.0047$			
Image-based rhizome VF	$\chi_{\text{rhiz}}=0.13$			
Syringodium filiforme				
No. of leaves, m	0	6	11	25
Resonator sound speed, c_{eff} (m/s)	410	400	396	375
Free-field sound speed, c_{o} (m/s)	1521	1175	1074	791
Apparent acoustic resonator VF, $V_{\text{air}}/V_{\text{tot}}$	0	3.49×10^{-5}	5.17×10^{-5}	1.38×10^{-5}
Acoustically-determined leaf VF	$\chi_{\text{leaf,a}}=0.0038$			
Image-based leaf VF	$\chi_{\text{leaf}}=0.24$			
No. of rhizomes, m	0	1	2	3
Resonator sound speed, c_{eff} (m/s)	408	402	398	393
Free-field sound speed, c_{o} (m/s)	1521	1275	1171	1066
Apparent acoustic resonator VF, $V_{\text{air}}/V_{\text{tot}}$	0	2.21×10^{-5}	3.55×10^{-5}	5.33×10^{-5}
Acoustically-determined rhizome VF	$\chi_{\text{rhiz,a}}=0.0032$			
Image-based rhizome VF	$\chi_{\text{rhiz}}=0.23$			
Halodule wrightii				
No. of leaves, m	0	10	21	33
Resonator sound speed, c_{eff} (m/s)	406	398	390	385
Free-field sound speed, c_{o} (m/s)	1519	1215	1008	946
Apparent acoustic resonator VF, $V_{\text{air}}/V_{\text{tot}}$	0	2.93×10^{-5}	6.55×10^{-5}	8.11×10^{-5}
Acoustically-determined leaf VF	$\chi_{\text{leaf,a}}=0.028$			
Image-based leaf VF	$\chi_{\text{leaf}}=0.19$			
No. of rhizomes, m	0	2	4	5
Resonator sound speed, c_{eff} (m/s)	410.3	407	406	403
Free-field sound speed, c_{o} (m/s)	1517	1358	1347	1244
Apparent acoustic resonator VF, $V_{\text{air}}/V_{\text{tot}}$	0	1.32×10^{-5}	1.42×10^{-5}	2.54×10^{-5}
Acoustically-determined rhizome VF	$\chi_{\text{rhiz,a}}=0.0021$			
Image-based rhizome VF	$\chi_{\text{rhiz}}=0.13$			

as represented by plant tissue volume fraction was also positively correlated with leaf and rhizome number [Figs. 3(a) and 3(b)] in *Thalassia* for both acoustic and image-based measurements. The image-based leaf (χ_{leaf}) and rhizome (χ_{rhiz}) void fractions were determined with the image analysis shown in Figs. 4 and 5. The image-based biomass was compared to the acoustic-based biomass measurement with the following relationship:

$$\left.\frac{V_{\text{leaves}}(m)}{V_{\text{tot}}}\right|_{\text{acoustic}} = \frac{V_{\text{air}}(m)}{V_{\text{tot}}}\frac{1}{\chi_{\text{leaf},a}} = \frac{\chi(m)}{\chi_{\text{leaf},a}}, \tag{2}$$

where $\chi_{\text{leaf},a}$ is the apparent leaf void fraction observed acoustically based on our previous hypotheses and m is the number of leaves. The same approach was applied to rhizome tissue. These calculations reveal a major difference between image- and acoustic-based biomass measurements, es-

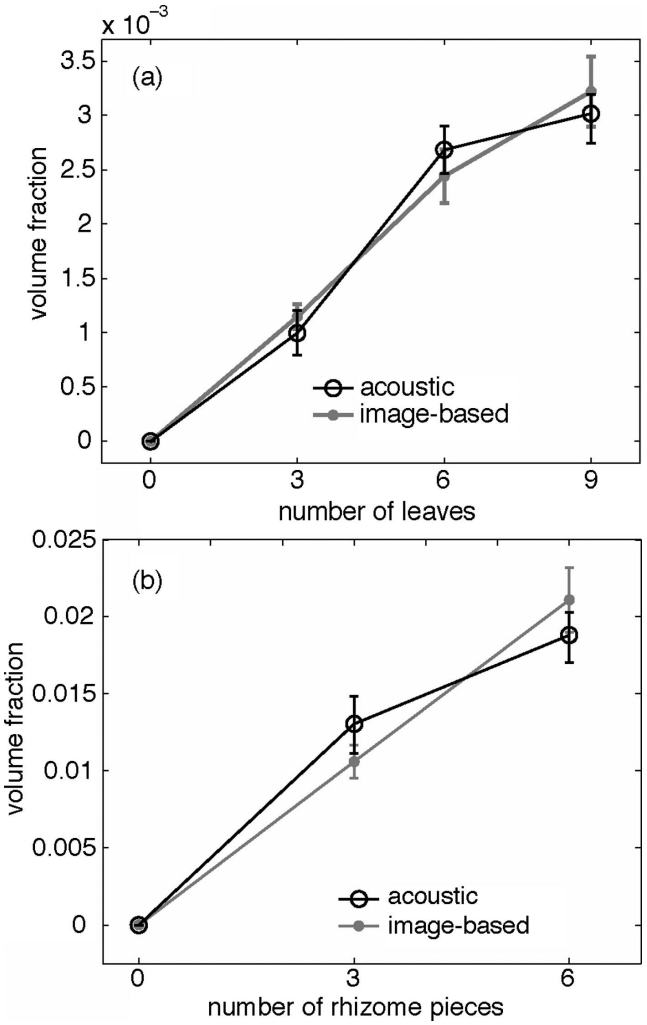

FIG. 3. *Thalassia testudinum.* Comparison of image- and acoustic-based biomass measurements as a function of the number of leaves (a) and rhizomes (b) in the resonator. The vertical axis is total volume fraction V_i/V_{tot} (i=leaves or rhizomes). The error bars are described in the text.

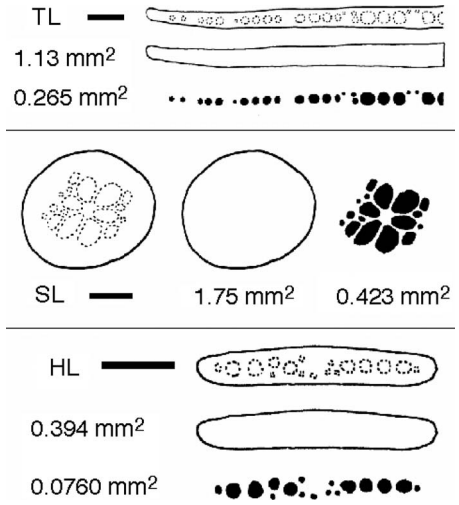

FIG. 4. Microscopic cross-sections of seagrass leaves (L) for *Thalassia* (T; top panel), *Syringodium* (S; middle panel), and *Halodule* (H; bottom panel). Since the cross-sections are nearly uniform perpendicular to the plane of the image, the void fraction is pore area/total area. Leaf sections adapted from Ref. 17. Only half the width of the leaf section is shown for TL. The aerenchyma are the circular features outlined with dashed lines or with black fill. Horizontal black scale bars are 0.5 mm in length. In each panel, the total leaf and pore area are shown adjacent to their corresponding images.

pecially in rhizomes (Fig. 3 and Table II). The best-fit values of $\chi_{\text{leaf},a}$ and $\chi_{\text{rhiz},a}$ (Table II) are means determined from the minimum and maximum values that allowed overlap of the error bars for all the points on both curves (Fig. 3). Such a fitting procedure was used because the curves go through the origin, and hence a linear least-squares approach (fitting only the slope) gave preferential consideration to the final point.

The error bars on the acoustic data represent the effects of uncertainty in the resonator length L and the finite resolution bandwidth of the spectrum measurement. The error bars on the image-based data are due to the finite resolution of the digital images. The leaves and rhizomes of *Thalassia* have extended shapes, where the length is much greater than the thickness. The primary uncertainty is in the accuracy of the thickness measurement, which was limited to about 2 pixels out of 20 in *Thalassi*a. The image-based leaf and rhizome void fractions are 6.8 and 28 times larger than the acoustically-determined void fractions (Table II).

The same procedure was repeated to obtain the physical properties, sound speeds, and void fractions of leaves and rhizomes for *Syringodium filiforme* and *Halodule wrightii* (Tables I and II). The cross-section imagery that yielded tissue void fraction appears in Figs. 4 and 5. The positive relationship between tissue (leaf or rhizome) abundance and volume fraction, as noted in *Thalassia* (Fig. 3), is also readily visible in *Syringodium* (Fig. 6) and *Halodule* (Fig. 7). As in *Thalassia*, however, comparison between the acoustic- and image-based biomass assessments in *Syringodium* and *Halodule* shows significant differences. For all three species, it is clear that biomass is directly proportional to the effective acoustic sound speed of the plant-filled water, but for *Syringodium*, the image-based leaf and rhizome void fractions are 63 and 72 times larger than the acoustically-determined void

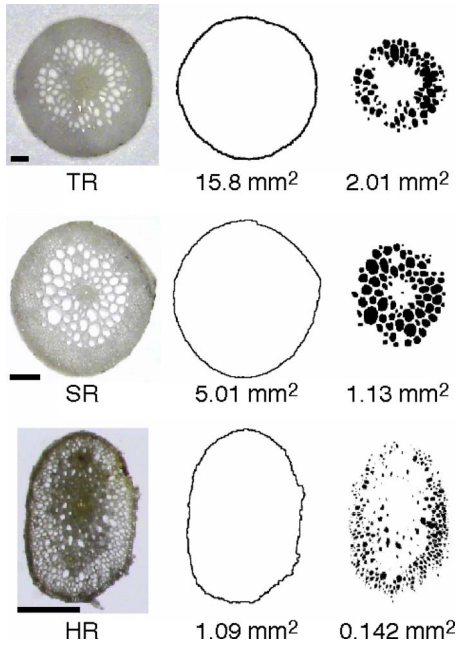

FIG. 5. (Color online) Microscopic cross-sections of rhizomes (R) for the three seagrass species. Abbreviations and notes as in Fig. 4.

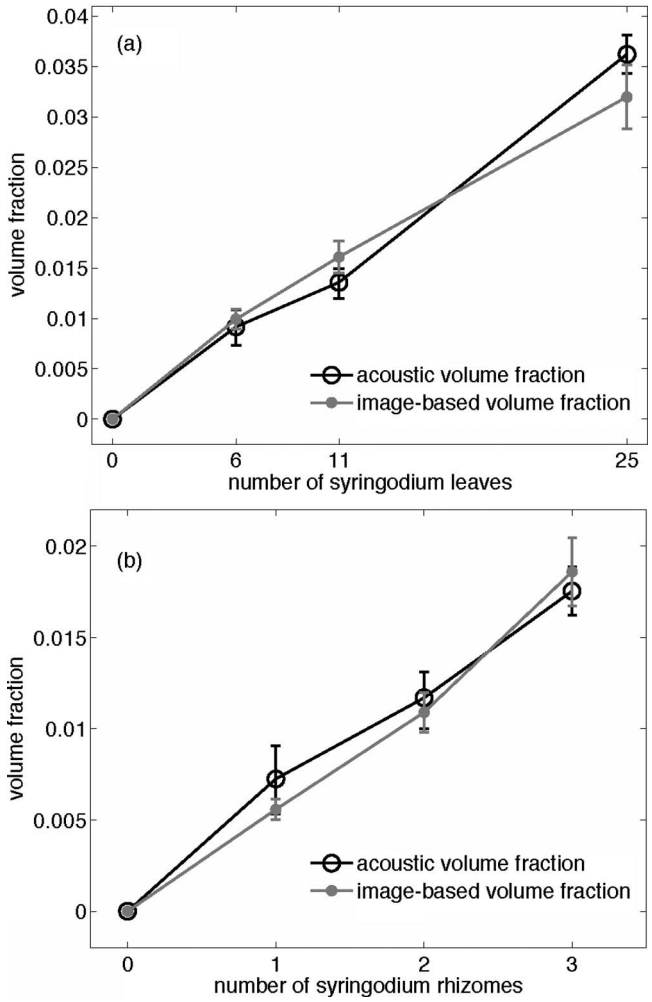

FIG. 6. *Syringodium filiforme*. Comparison of image- and acoustic-based biomass measurements as a function of the number of leaves and rhizomes in the resonator. The vertical axis is total volume fraction V_i/V_{tot} (i =leaves or rhizomes). The error bars are described in the text.

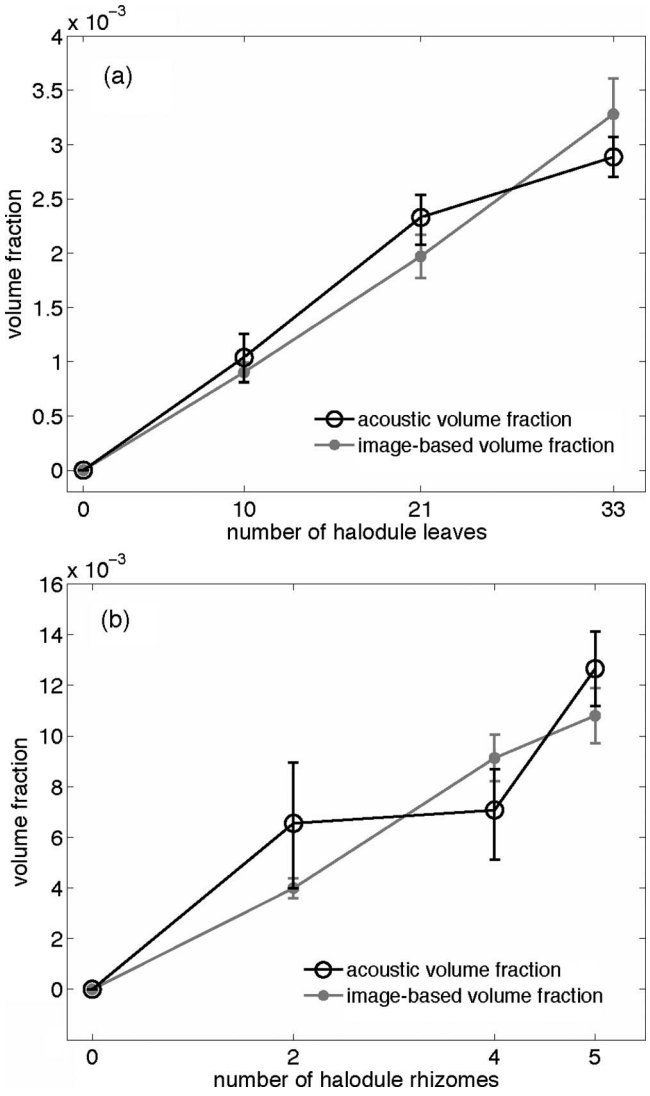

FIG. 7. *Halodule wrightii*. Comparison of image- and acoustic-based biomass measurements as a function of the number of leaves and rhizomes in the resonator. The vertical axis is total volume fraction V_i/V_{tot} (i=leaves or rhizomes). The error bars are described in the text.

fractions (Table II). In *Halodule*, the image-based leaf and rhizome void fractions are 6.8 and 62 times larger than the acoustically-determined void fractions (Table II).

A comparison of the ratio of the image-based to acoustically-determined void fractions for both leaves and rhizomes of all three species reveals some interesting differences (Fig. 8) that reflect the acoustic importance of the tissue. A ratio of unity indicates plants that behave acoustically like air bubbles in water. An increasing ratio indicates increasing tissue stiffness, which effectively reduces the acoustic contrast of the internal gas and thereby reduces the acoustic contrast of the plant. For all three species, the rhizome tissue is stiffer than the leaf tissue, and there is a large difference between the two tissues for both *Thalassia* and *Halodule*. *Syringodium* exhibits the highest tissue stiffness of the three species, and the leaf and tissue stiffness is of similar magnitude. The high stiffness of *Syringodium* leaves may be explained by the cylindrical shape of its above-ground photosynthetic tissues. Volumetric excitation of the pore space places the circumferential tissue in tension, with hoop-like structures resisting expansion. For all three species, the rhizomes are circular in cross-section with internal gas-filled pores, similar to *Syringodium* leaves. In contrast, the leaves of *Thalassia* and *Halodule* are flat and there is little tissue to resist the expansion.

The three species examined here exhibit significantly different acoustic-based and image-based void fractions. Since the image-based void fractions are from direct observations of the plant structure, they were considered to be the best estimate of the actual plant void fraction. One must therefore conclude that hypotheses (1) and (2) are incorrect. Wood's equation is insufficient and the acoustic response of all three species (*Thalassia testudinum*, *Syringodium filiforme*, and *Halodule wrightii*) is dependent on both gas content and the tissue acoustic properties. This corroborates a similar result Hermand[3] found *in situ* for *Posidonia oceanicus.*

There are a number of potential differences between the *in vitro* response observed in the present work and the *in situ* response. First, these experiments were conducted under sufficiently low light conditions to prevent the appearance of bubbles on the leaf surfaces, which indicates that photosyn-

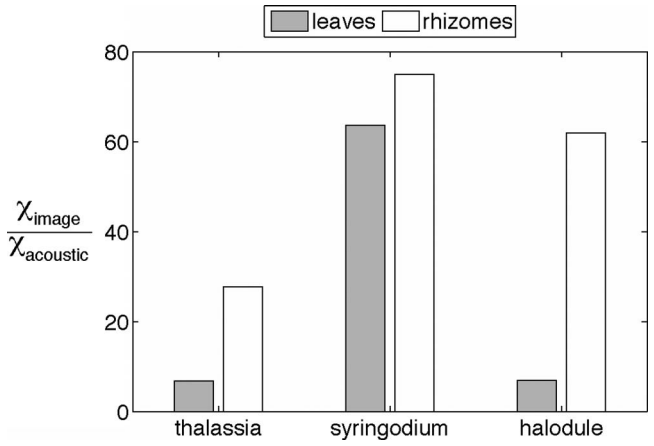

FIG. 8. The ratio of the image-based to acoustically-determined void fractions for both leaves and rhizomes of each species. This ratio is a measure of the importance of the tissue acoustic parameters. A ratio of unity indicates plants that behave acoustically like air bubbles in water. An increasing ratio indicates increasing tissue stiffness, which effectively reduces the acoustic contrast of the internal gas and also reduces the acoustic contrast of the plant.

thetic respiration was not underway during the experiments. *In situ*, under different light conditions and hence, different photosynthetic respiration conditions, the acoustic response of all three species will likely be different because the gas content and internal pressure of the plant will be different. A limited number of measurements under light saturation conditions were conducted and significant bubble production on the leaves of *Thalassia* was observed, which in turn further reduced the effective resonator sound speed, as expected. This was accompanied by a significant temperature increase in the resonator to unnaturally high levels. Resonator temperature control will have to be implemented in the present apparatus to accurately investigate the effect of illumination level. Second, the results reported here are for near-surface conditions. Because the sound speed in a gas is dependent on the ambient pressure, the acoustic response of seagrass will also be a function of depth. Third, during the present experiments, the acoustic axis was oriented along the length of the leaves whereas *in situ*, the acoustic axis could be oriented perpendicular to the leaves. Since some seagrass species have long, thin, relatively flat leaves, there is likely an excitation frequency above which the effective acoustic properties for cross-leaf propagation may be a function of leaf orientation. Despite these complexities, this work shows that seagrass biomass is directly related to the low frequency effective sound speed in a body of water containing seagrass plants. Further, the ability to remotely detect gas content in both above- and below-ground tissues may provide a reliable technique to rapidly assess photosynthetic production in seagrass beds that are chronically exposed to limiting light conditions in estuarine environments.[3,7,14]

VI. CONCLUSIONS

The low frequency acoustic properties of seagrass leaves and rhizomes were investigated *in vitro* using an acoustic resonator technique and image-based biomass measurements. The effective sound speed inside a plant-and-water-filled resonator was found to be proportional to overall tissue biomass contained in the resonator. The effective sound speed decreased as the number of leaves (or rhizome pieces) increased. The change in sound speed was reduced for physically smaller leaf species ($Halodule < Syringodium < Thalassia$). Gas content is clearly important, but since gas content (via Wood's equation) by itself did not describe the observed sound speeds, the acoustic response of the tissue must also be considered in the development of future acoustic models of sound propagation in seagrass beds. Finally, we found that flat leaves exhibited more acoustic contrast than did circular cross-section leaves or rhizomes, potentially due to hoop stress in the outer layers of the circular cross-section tissues characteristic of *Syringodium*.

The present work is a first step toward modeling sound propagation in seagrass beds. Additional work is needed to fully understand even the simplified laboratory experiments reported here. Significant additional work is needed to understand the complexities mentioned above and additional complexity found *in situ*, such as diurnal and seasonal variations.

ACKNOWLEDGMENTS

We thank K. Jackson for providing fresh samples of field-collected seagrasses and Chad Greene for assistance with the image analysis. Work supported by the Office of Naval Research Ocean Acoustics Program, the UT College of Engineering, and the Texas Sea Grant College Program Grant No. R/ES-87.

[1]E. M. McCarthy and B. Sabol, "Acoustic characterization of submerged aquatic vegetation: Military and environmental monitoring applications," in *Proceedings of OCEANS 2000 MTS/IEEE Conference and Exhibition* (IEEE, Piscataway, NJ, 2000), Vol. **3**, pp. 1957–1961.
[2]A. P. Lyons and D. A. Abraham, "Statistical characterization of high-frequency shallow-water seafloor backscatter," J. Acoust. Soc. Am. **106**, 1307–1315 (1999).
[3]J. P. Hermand, in *Handbook of Scaling Methods in Aquatic Ecology: Measurement, Analysis, Simulation*, edited by L. Seuront and P. G. Strutton (CRC, Boca Raton, FL, 2004), pp. 65–96.
[4]V. Pasqualini, P. Clabaut, G. Pergent, L. Benyoussef, and C. Pergent-Martini, "Contribution of side scan sonar to the management of Mediterranean littoral ecosystems," Int. J. Remote Sens. **21**, 367–378 (2000).
[5]P. J. Mulhearn, "Mapping seabed vegetation with sidescan sonar," DSTO Report No. TN-0381, Defence Science and Technology Organization, Australia, 2001.
[6]T. Komatsu, C. Igarashi, K. Tatsukawa, S. Sultana, Y. Matsuoka, and S. Harada, "Use of multi-beam sonar to map seagrass beds in Otsuchi Bay on the Sanriku Coast of Japan," Aquat. Living Resour. **16**, 223–230 (2003).
[7]J. P. Hermand, P. Nascetti, and F. Cinelli, "Inversion of acoustic waveguide propagation features to measure oxygen synthesis by Posidonia oceanica," in *OCEANS '98 Conference Proceedings* (IEEE, Piscataway, NJ, 1998), Vol. **2**, pp. 919–926.
[8]A. B. Wood, *A Textbook of Sound*, 1st ed. (MacMillan, New York, 1930).
[9]R. C. Phillips and E. G. Meñez, *Seagrasses* (Smithsonian Institution Press, Washington, DC, 1988).
[10]P. S. Wilson, "Low-frequency dispersion in bubbly liquids," ARLO **6**, 188–194 (2005).
[11]P. S. Wilson, A. H. Reed, J. C. Wilbur, and R. A. Roy, "Evidence of dispersion in an artificial water-saturated sand sediment," J. Acoust. Soc. Am. **121**, 824–832 (2007).
[12]P. S. Wilson, R. A. Roy, and W. M. Carey, "Phase speed and attenuation in bubbly liquids inferred from impedance measurements near the individual bubble resonance frequency," J. Acoust. Soc. Am. **117**, 1895–1910 (2005).
[13]J. S. Bendat and A. G. Piersol, *Engineering Applications of Correlation and Spectral Analysis*, 2nd ed. (Wiley, New York, 1993).

[14]K. H. Dunton, "Seasonal growth and biomass of the subtropical seagrass *Halodule wrightii* in relation to continuous measurements of underwater irradiance," Mar. Biol. (Berlin) **120**, 479–489 (1994).
[15]N. P. Fofonoff, "Physical properties of seawater: A new salinity scale and equation of state for seawater," J. Geophys. Res. **90**, 3332–3342 (1985).
[16]National Oceanographic Data Center, "Coastal water temperature guide–Gulf of Mexico Coast: Western," http://www.nodc.noaa.gov/dsdt/cwtg/wgof.html (Last viewed April, 2008).
[17]R. C. Phillips and C. P., McRoy, *Handbook of Seagrass Biology: An Ecosystem Perspective* (Garland STPM, New York, 1980).
[18]V. A. Del Grosso, "Analysis of multimode acoustic propagation in liquid cylinders with realistic boundary conditions—Application to sound speed and absorption measurements," Acustica **24**, 299–311 (1971).